Final Report

NASA Grant NGR 05-007-327

Magnetometer Instrument Team Studies for the Definition Phase of the Outer Planets Grand Tour

Principal Investigator: Paul J. Coleman, Jr.

Space Science Center
Institute of Geophysics and Planetary Physics
University of California
Los Angeles, California 90024

March 21, 1973

I. INTRODUCTION

This document is the final report on the work performed by the magnetic fields investigation team during the mission definition phases of the Outer Planets Grand Tour (OPGT) and the Mariner Jupiter Saturn (MJS) Missions. This work involved three tasks: defining the objectives of the magnetic fields investigations, defining the magnetometer systems required to meet these objectives, and developing and testing hardware elements in certain mission-specific areas.

II. TEAM MEMBERSHIP AND STRUCTURE

The magnetic fields investigation team is organized into three groups. One is concerned with the scientific aspects of missions to the outer planets and the other two are concerned with the instrumentation required for magnetic field investigations on such missions. The activities of these three groups were co-ordinated by the team members at UCLA with the assistance of the staff there. The UCLA people also supported those activities of the team leader that were directly related to his participation on the Science Steering Group for the Outer Planets Grand Tour (OPGT) and Mariner Jupiter Saturn (MJS).

The members of the team are:

Ames Research Center

Dr. David S. Colburn, Deputy Team Leader
Mr. Carle Privette
Dr. Charles P. Sonett

Brigham Young University

Professor Douglas E. Jones

California Institute of Technology

Professor Leverett Davis, Jr.

Imperial College of Science and Technology

Professor Harry E. Elliot
Dr. Peter Hedgecock

Jet Propulsion Laboratory

Mr. A. Frandsen
Mr. G. Reisdorf
Dr. E.J. Smith

University of California, Los Angeles

Professor Paul J. Coleman, Jr., Team Leader
Mr. Robert C. Snare

University of Chicago

Professor Eugene Parker

University of Newcastle upon Tyne

Professor S. Keith Runcorn

III. SUMMARY OF TEAM ACTIVITIES

During the period April-December, 1971, the magnetometer team defined the objectives of magnetic field investigations on missions to the outer planets, defined an instrumentation system with which to accomplish these objectives, proposed a program of studies and instrument development tasks for the mission definition phase of the Outer Planets Grand Tour (OPGT) project, and undertook the execution of this program.

The team also established requirements for the spacecraft and the mission which would insure their compatibility with the magnetic field investigation proposed for the outer planets missions and developed figures of merit for encounter trajectories. Finally, the team, in collaboration with the OPGT Project Office, worked to define the spacecraft-instrumentation interface and the on board data handling system. This OPGT work is, for the most part, covered in various working papers and reports by the team, by the Science Steering Group (SSG), and by the OPGT Project Office at JPL.

During the period January-April, 1972, the team participated in defining the program for exploring the outer planets within the more restrictive constraints of the Mariner Jupiter Saturn (MJS) mission. This task included defining a suitably limited magnetic fields investigation as well as re-examining and modifying as required the results of the OPGT work described in the preceding paragraph. This MJS work is covered in previous reports by the various groups including the team, the SSG, and the Project Office.

IV. THEORETICAL STUDIES

The theoretical studies of the team were directed toward modeling the magnetic environments of the outer planets and their satellites and the outer heliosphere. The purpose of these tasks was to establish performance specifications and requirements for the instrumentation, spacecraft, and mission procedures and to determine the relative merits of the achievable trajectories for the magnetic field investigations on OPGT. Likely methods of data analysis were also studied so that any resulting requirements on the instrumentation and data handling system could be established.

At CIT, a program was written and tested that will determine the magnetic multipole moments of a planet such as Jupiter from observations made on a parabolic trajectory. It was proved possible to determine all dipole and quadrupole terms from observations made in a plane and it appears virtually certain that with good data the octupole terms can also be determined. The program also determines the rotation rate of the hidden core in which it is assumed the sources are fixed and the spherical harmonic coefficients in the expansion of the contribution to the field by external sources such as currents in the magnetopause.

Programs were also written and tested to generate adequately accurate hyperbolic trajectories corresponding to a variety of possible flybys and to generate artificial test data for each. This test data, based on assumed sources and rotation rates of the core, can then be analyzed by the basic program. In this way it can be determined which of a variety of possible trajectories allows the most accurate determination of the multipole moments.

These programs will be useful in determining the accuracy that can be expected with varying amounts of noise in the data but will be less useful with MJS than with the Grand Tour because with fewer alternative launch times and missions contemplated, there are fewer alternatives among which to choose, and what choices there are are usually dictated by other considerations.

The theoretical/model studies at ARC and Newcastle were adequately covered in the team report dated May 1.

V. INSTRUMENT DEVELOPMENT

In order to insure the availability of instrumentation suitable for the proposed magnetic fields investigations on missions to the outer planets, several instrument development tasks were undertaken by the team. The objectives are to analyze and test modified state-of-the-art magnetometers in order to identify any modifications and improvements that would be desirable for such missions.

Two types of magnetometers were examined in this study, the vector fluxgate magnetometer and the vector helium magnetometer. The test-model fluxgates are ones designed at the Ames Research Center and incorporating ring core sensors designed at the Naval Ordnance Laboratory and then fabricated by Schonstadt Instrument Co. for Imperial College. The test-model helium magnetometer is a modification of one developed at the Jet Propulsion Laboratory for Pioneer/Jupiter.

Procedures for simulating the radiation environments of the missions were developed, prototypical instruments or components thereof were tested and their respective designs received to see how their reliability and radiation resistance might be improved. This work is covered in the team report dated May 15, 1972.

A detailed description of the fluxgate test unit used at ARC is contained in Appendix I.

Additional studies of the vector helium sensor were performed by BYU and JPL. All of the experimental work was performed using the facilities at JPL and the analysis was performed both at JPL and at BYU.

The objectives of our study program, as performed in conjunction with JPL personnel, included the following:

1. Empirical and theoretical studies of cell and lamp parameters affecting the ultimate sensitivity of the helium instrument.

2. Empirical and theoretical studies of the factors affecting the zero field offset other than those caused by thermoelectric currents.

In both of the above study areas, we attempted to understand the fundamental physics of all mechanism involved so that predictions could be made with some confidence. As a result of our efforts, the BYU/JPL team was able to develop a specific sensor design having the characteristics that were as good or better than those outlined as goals in the beginning of this program.

Our theoretical/analytical studies included work in the following specific areas:

1. High sweep field offset in the x-z and x-y sweep modes. In general, for the x-z mode we find

$$H_{ax} = [2\beta^2/K(4\beta-z)\cdot H_s V_x(f_o) \sim [2V_x(f_o)/K]H_s$$

for H_s large (i.e., $\beta\to 1$, $\alpha\to 0$). Here, H_{ax} is the effective offset field in the x direction as a function of the fo modulation signal Vx(fo). The parameters α and β are given by

$$\alpha = H_{ax}^2 + H_{ay}^2/H_s^2$$

$$\beta = 1 + (H_o^2/H_s^2) + (H_A^2/H_s^2)$$

with H_o = an equivalent field related to the metastable helium relaxation time, H_A = the total ambient field, H_s = the sweep frequency. For the x-y sweep mode this becomes

$$H_{ax} = [\beta^2/2K(\beta-\alpha-1)]H_s V_x(f_o) \sim H_s^3 V_x/2KH_o^2$$

This analysis suggests that for high field operation (high sweep field unless the adaptive mode is used) the x-y mode should only be used on the lowest scales.

2. Spectral measurements of D_0 and D_3 light versus lamp pressure and power. A 1.8 meter Jarrell-Ash grating spectrophotometer was used to measure the intensity of the D_0 and D_3 light from a number of Pioneer type lamps filled at different pressures and operated over a range of matched input powers. These data suggested an empirical fit of the form

$$S = A(1 - e^{-\alpha(P/P_o)^\beta})e^{-\alpha(P/P_o)^\beta}$$

The parameters exhibiting a best fit to the data were A = 12.6, $\alpha = 0.692$, $P_o = 5.5$ mm Hg and $\beta = 1.28$. Test data obtained prior to this study period by other JPL personnel suggested a possible dependence of light output efficiency on lamp element diameter, but we were unable to conduct a detailed analysis program to pursue this effort further. However, it was possible to establish an optimum lamp pressure for the Pioneer lamp configuration.

3. H_0 and the electron collision time Γ_e. We were able to measure the effective collision time in the cell discharge by means of a new technique using the parameter H_0 found in the magnetometer signal expression developed by B. Connor. The parameter H_o is given by $H_o = 1/\gamma\Gamma_r$, where Γ_r is the metastable relaxation time and γ is the magnetogyric ratio. The expression by Conner is

$$V(t) = K[H^2(t) \sin^2 \theta(t)/H_o^2 + H^2(t)]$$

Here K is the peak amplitude (large sweep field) of the second harmonic and H_o is obtained by measuring the sweep field magnitude corresponding to $V(2f_o) = K/2$. Our study has shown that the effective collision time, Γ_c, in the 1.5 mm Hg cell is about 0.12 milliseconds which strongly suggests collisions between the metastables and hot (4 ev) electrons as opposed to wall collisions.

4. The theoretical dependence of K/H on pumping light. The quantity K/Ho is a basic measure of the ultimate responsitivity of the helium instrument that relates to the physical processes in the cell itself that results from the collisional and pumping process in the cell. We found that

$$K/H_o = \alpha\beta\Gamma_c/1 + (\alpha/D_o\Gamma_c)$$

where α is a parameter that depends upon the atomic cross section, etc., D_o is the intensity of the D_o component of the I.R. pumping light, β is a parameter relating K to D_o and Γ_c the effective collision time. We found excellent agreement between the shape of the predicted curve and that measured in the laboratory.

5. Ultimate frequency response of the helium instrument as a result of the pumping and depumping times. Measurements and theory suggest maximum sweep frequencies of the order of 5-10 KHz.

6. Offset changes versus cell and lamp power, and sweep amplitude and frequency.

7. Noise spectrum measurements, ultimate sensitivity versus sweep frequency.

8. Measurement of the shift in the magnetic center versus discharge configuration.

9. Determination of the cell length versus cell pressure for peak signal to noise. In this program a theoretical expression was derived relating the minimum cell power optical pumping signal to the corresponding cell opacity and a fit obtained to the experimental data. As a result, it was possible to determine the optimum cell length corresponding to that cell pressure for which a reasonable ignition voltage was required.

10. A measurement of the effect of cell discharge geometry on sensor sensitivity.

11. The fundamental minimum offset due to the interaction of the magnetic moments of pumped helium atoms with the rotating magnetic field in the presence of sweep and ambient field gradients. A theoretical study of the interaction of the magnetic moments of helium atoms with the rotating sweep field has resulted in a self-consistent explanation of the offset measurements conducted in both the cryogenic flux tank and the mu-house. Other predictions of this mechanism have not been checked out as of yet.

12. As a result of a theoretical study of the sensitivity achievable in the transverse sweep or x-y mode a cross-cell sensor has been proposed incorporating the optimum cell length-pressure relationship. This sensor should permit operation with a sensitivity of better than 1 milligamma rms on all three axes. Verification tests have not been obtained as yet, although 1 milligamma operation in the x-z mode with a standard cylindrical cell of optimum length has been achieved at optimum sweep magnitude by JPL personnel.

Appendix I

FLUXGATE TEST UNIT

by

Michael G. Dix
NASA Ames Research Center
Moffett Field, Ca. 94035

V-6

Introduction

The proposed mission to Jupiter and Saturn by a Mariner spacecraft in 1976 will include a magnetometer which is to be capable of measuring both the low fields of interplanetary space (5-10 milligamma) as well as the high fields expected in the vicinity of Jupiter (.1-1 gauss). The fluxgate magnetometer is a good contender for this application since the inherent simplicity, large dynamic range and proven reliability of the fluxgate instrument are well known.

A study program to determine the resolution of the fluxgate sensor was established to see if the scientific requirements of the mission could be met by the fluxgate instrument. The main goal of the study program was to see if the fluxgate could detect milligamma fields while exhibiting long term stability.

Fluxgate Test Unit

In the critical evaluation of ring core fluxgate sensors it was suspected that the drifts and noise previously thought to have their origin in the sensor were in fact due to the associated electronics. With this in mind, an electronic test set was developed to overcome the more obvious sources of drift and noise.

Fluxgate sensor drift can be caused by variations in the drive signal. Frequency drift in the drive signal shows up as a phase shift in the sense winding signal output producing apparent drift. The use of a crystal controlled timing circuit eliminates this effect. Sensor drift can also be caused by the change of second harmonic content of the drive signal. This effect is minimized by using amplifiers with a high degree of feedback and complementary matching drive transistors. High frequency noise can be caused by noise in the drive amplifier. Drive amplifier noise reduction is achieved by running each drive amplifier stage at low gain and well within their operating range.

High frequency noise in the sensor output also can be minimized by using a sense winding amplifier having a minimum bandwidth and using low noise amplifiers.

Both offset and noise can be caused by the sense signal demodulator and following integrating amplifier. In the fluxgate test unit special care was used in the design of each of these stages though no unusual techniques were used.

The overall design of the fluxgate test unit follows conventional designs which have been used numerous times in space; however, through the use of the techniques mentioned above and through the use of recently developed integrated circuits a significant improvement was observed over previous designs. For example, drifts previously attributed to the sensor of 0.1 gamma or so were not seen with the test unit, peak-to-peak noise at 10 Hz was reduced and apparent instabilities in the flux tank were no longer seen.

Circuit Design

The fluxgate test unit follows conventional design techniques as can be seen from the block diagram of Figure 1. The drive winding of the sensor is driven at 5 kHz and the second harmonic signal from the sense winding is filtered and amplified by a narrow band AC amplifier centered at 10 kHz. The output of the AC amplifier is demodulated by a pair of inverted transistor switches.

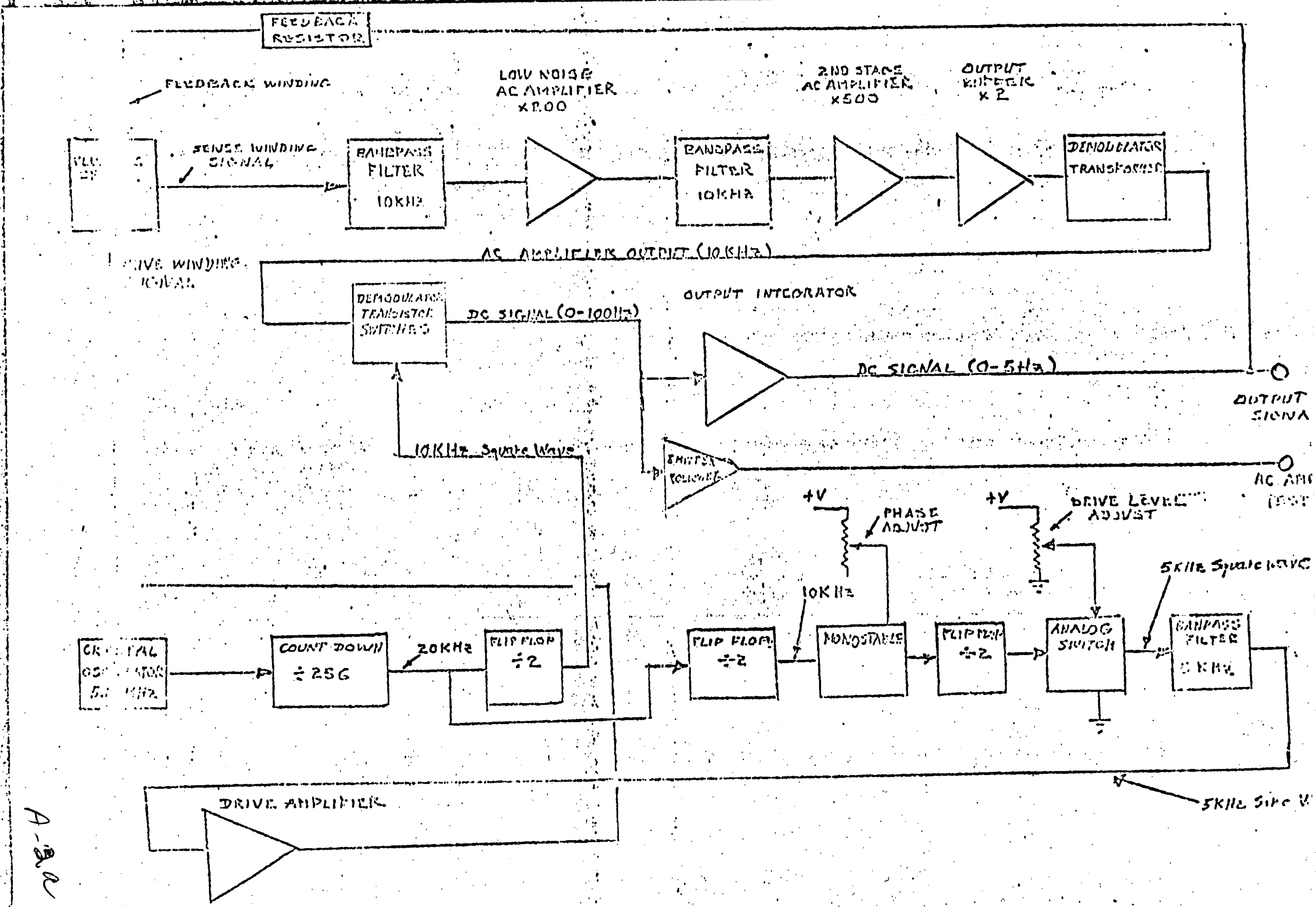

A-2a

FLUXGATE TEST UNIT

The low frequency signal from the demodulator is amplified by an integrating amplifier with a frequency of 5 Hz. The integrating amplifier output is used to provide feedback signals to the sensor and is used as the unfiltered output of the test unit.

A crystal oscillator and associated count down circuits provide the timing for the test unit. Demodulator switching signals are taken directly from the timing chain while the drive signal timing is delayed by an adjustable monostable to allow for phase adjustment of the demodulator phase with respect to the drive signal.

All components used in the fluxgate test set were selected to be interchangeable with commonly available parts used for space flight programs.

Narrowband AC Amplifier

The AC amplifier has three gain stages and two bandpass filters. Signals from the sense winding of the fluxgate sensor are passed through the first bandpass filter stage to eliminate any drive signal from the input to the first AC amplifier stage. Drive signal components appearing at the first amplifier can cause distortion thereby producing apparent offset in the sensor. The first AC amplifier is a LM725 low noise integrated circuit amplifier operated at a gain of 200. The output of this amplifier is passed through the second bandpass filter further removing any spurious signals from the sensor and limiting the frequency content of the sensed signal. The second AC amplifier, a LM725, has a gain of 500. Both the first and second AC amplifier are compensated to give a total stable gain of 700 dc at 10 kHz. A third amplifier, an output buffer, isolates the second amplifier from the demodulator switching transistors. This amplifier, a LM301, is connected as a voltage follower with a gain of two. The bandpass filters used for the AC amplifier have a 100 Hz bandpass at 10 kHz. To avoid phase shift due to the filters the first stage filter has a leading phase characteristic and the second filter a lagging characteristic. The two filters in cascade then have a phase shift of less than 60° over the bandpass. Figure 2 shows the AC amplifier gain versus frequency performance. The schematic for the AC amplifier shown in Figure 3.

Drive Amplifier

The drive amplifier shown in Figure 4 is capable of providing up to one amp peak current to allow driving a number of different types of ring core sensors. Special care is taken in the drive amplifier to eliminate second harmonic distortion by using a complementary output stage and power supply decoupling. Two 709 operational integrated circuits are used rather than a single amplifier to minimize drive signal distortion and noise. The first drive amplifier acts as an impedance matching circuit for the drive bandpass filter and the second amplifier drives the complementary compound emitter follower used in the output circuit. The sine wave signal for the drive amplifier is generated by passing the output of an analog switch, a square wave, through a 5 kHz bandpass filter. The analog switch timing is derived from the timing chain. Drive level is adjusted by controlling the DC level to the analog switch. Adjustment of the DC level to the analog switch rather than changing the gain of either drive amplifier stage prevents any change in frequency characteristics

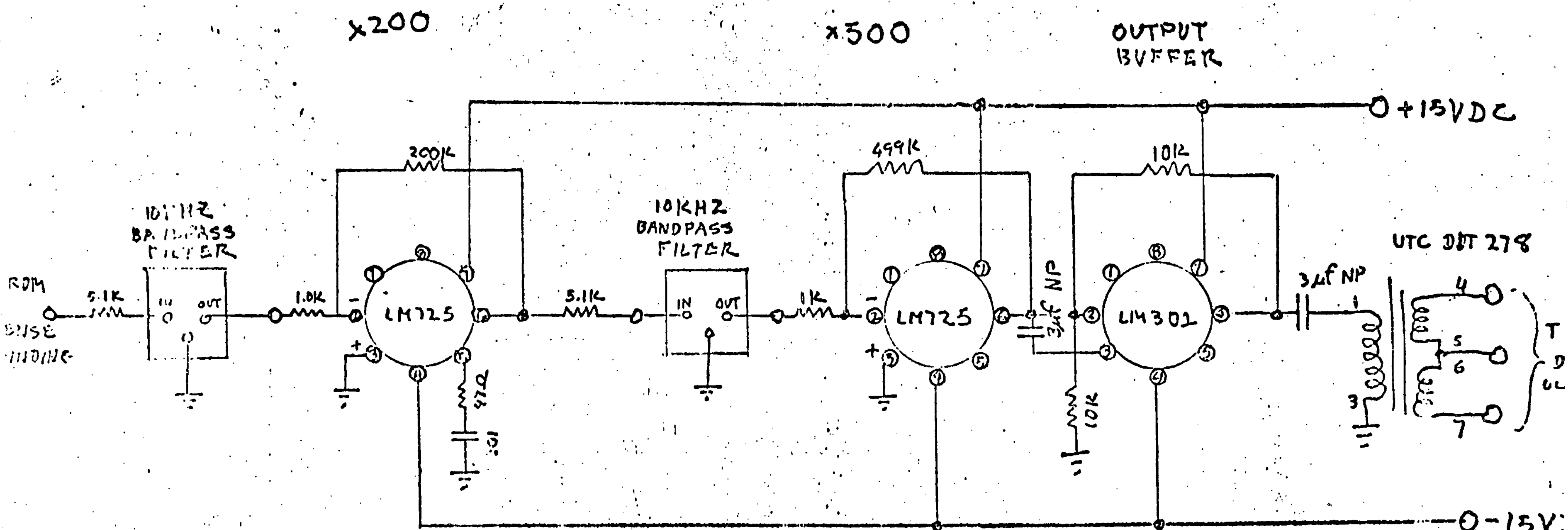

NARROW BAND AMPLIFIER

FIGURE B

A-4-a

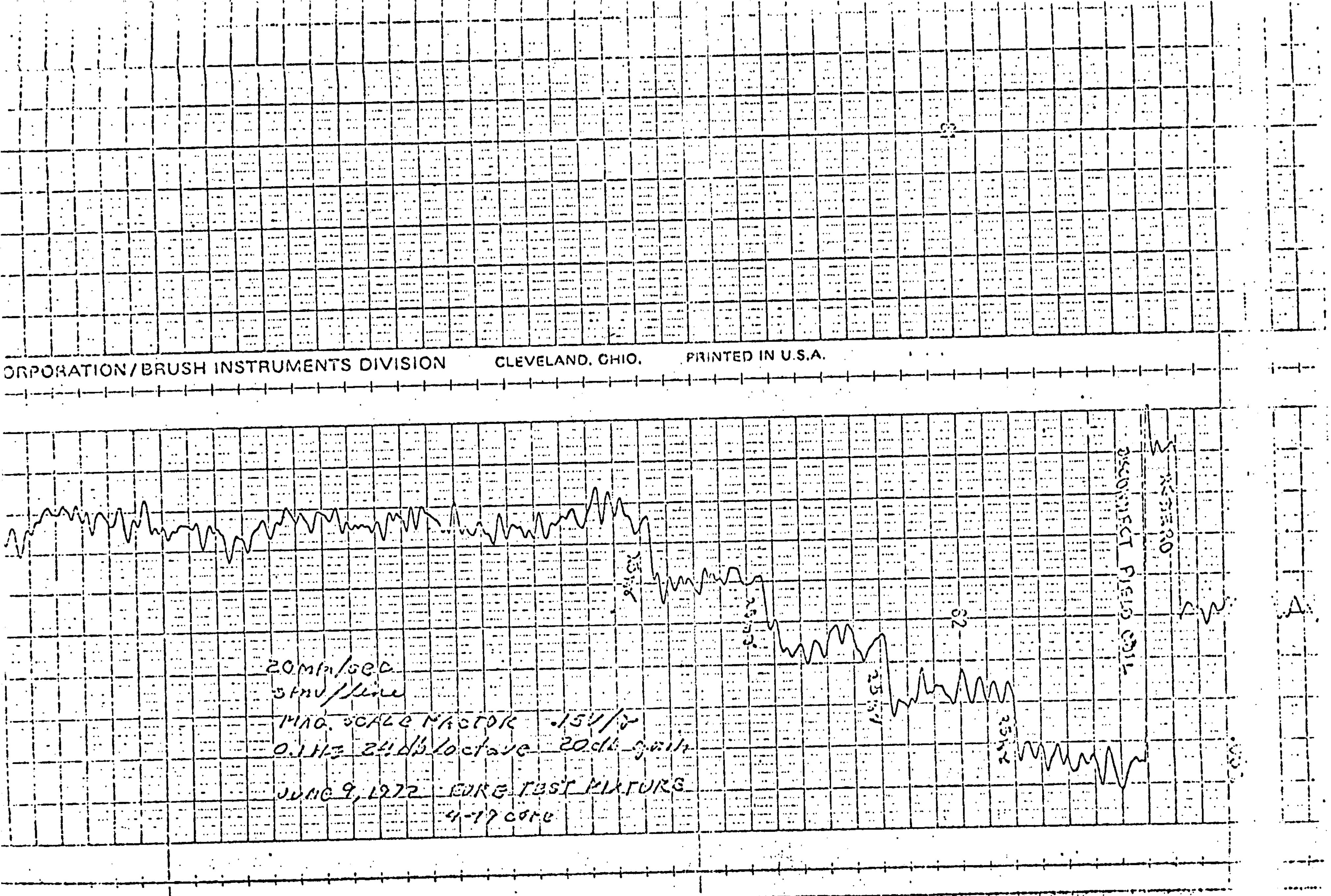

ORPORATION/BRUSH INSTRUMENTS DIVISION
CLEVELAND, OHIO.
PRINTED IN U.S.A.
20mm/sec
5mV/line
MAG. SCALE FACTOR
0.1Hz 24db/octave 20db gain
JUNE 9, 1972 CORE TEST FIXTURE
4-17 core
DISCONNECT FIELD COIL
RE-ZERO

FIGURE 3

A-4-6

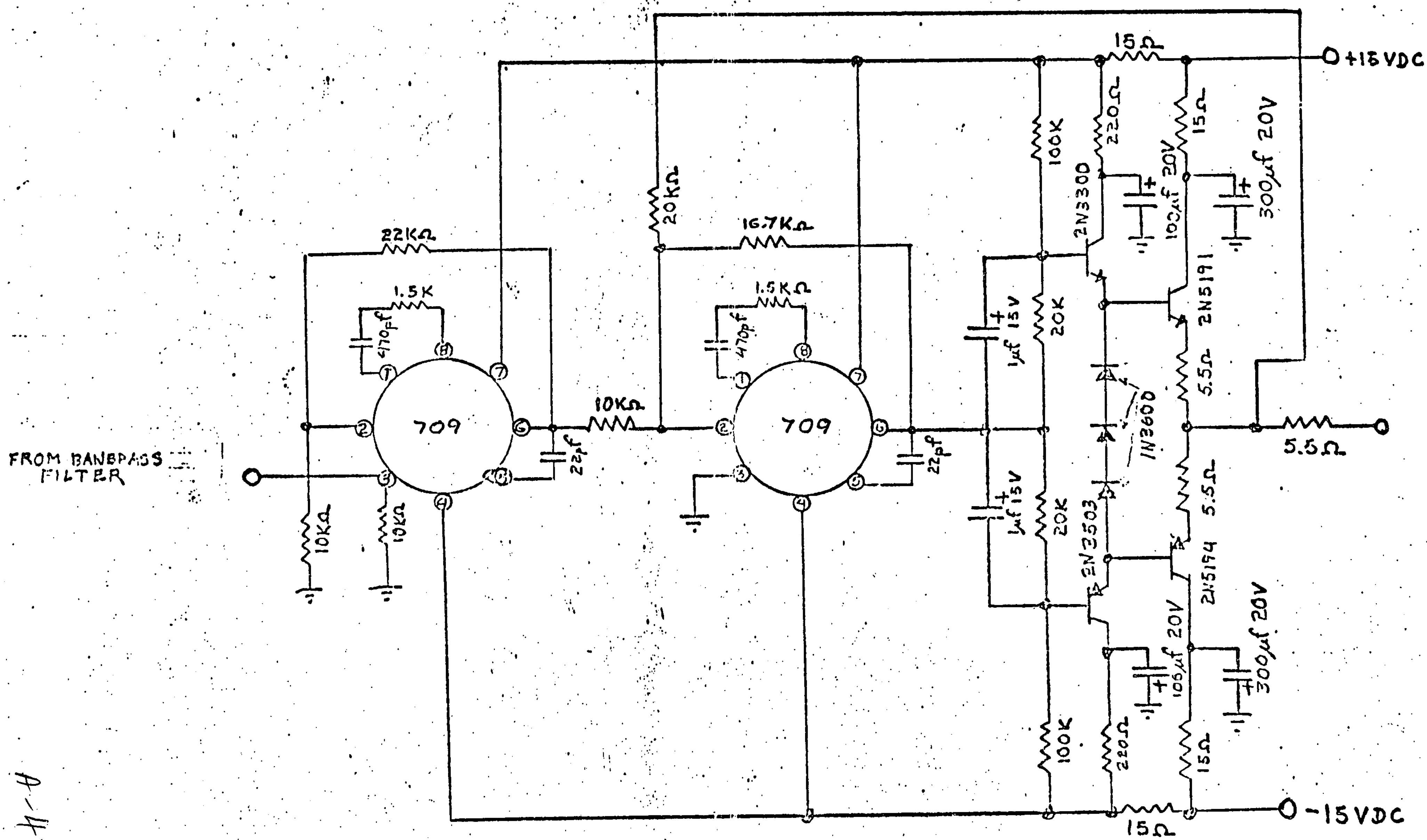

DRIVE AMPLIFIER

FIGURE 4

A-4-C

of the overall drive amplifier.

Timing and Logic Circuits

The primary timing of the instrument comes from a 5.12 MHz crystal followed by a count down of 256. The resultant 20 kHz signal is divided by two by a JK flip flop producing two 10 kHz symmetric square waves opposite in phase. The 10 kHz signals drive the demodulator switches. The drive signal timing is produced by dividing the 20 kHz signal by 2 and passing the resulting 10 kHz through an adjustable monostable multivibrator. The phase of the drive signal is adjusted by changing the delay of the output of the monostable. The output of the monostable is divided by two by a JK flip flop to produce a symmetric 5 kHz square wave. This square wave drives the analog switch which cops the DC drive level voltage into a square wave for the bandpass filter. The schematic for the timing and logic is shown in Figure 5.

Output Integrator

The output integrator, Figure 6, is a pair of integrated circuit amplifiers (LM 725 and NH0002) which are used to amplify the demodulator output signal to an instrument output of ± 5 volts full scale. The LM725, balanced for low DC drift with temperature, drives a NH0002 emitter follower. The use of the output emitter follower on the integrator amplifier prevents loading due to external test equipment. Sensor feedback signals are taken from the emitter follower output also. The integrator acts as a low pass amplifier with a frequency cutoff at 5 Hz. The principal time constant of the test unit is set by the integrator time constant.

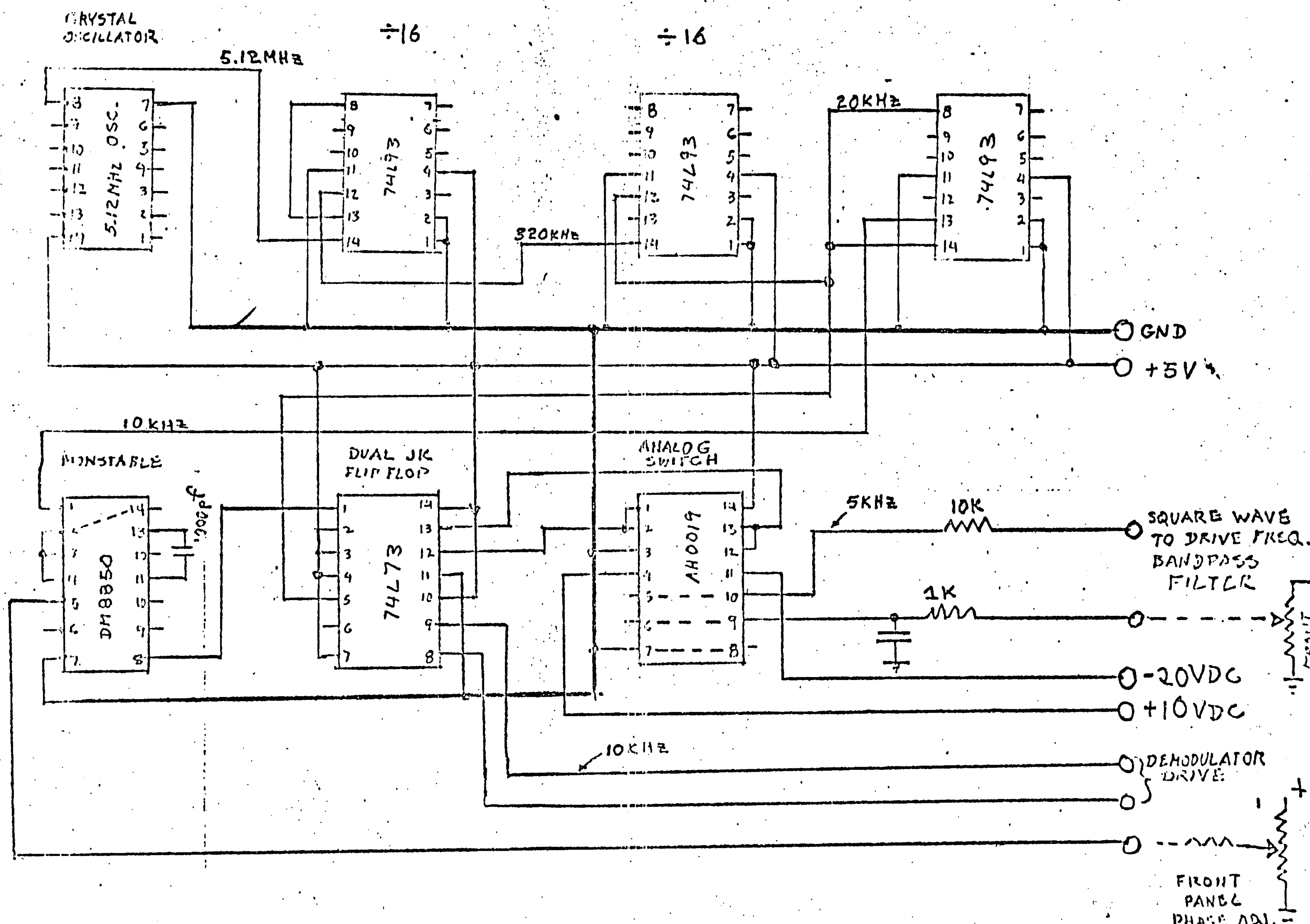

TIMING AND LOGIC CIRCUIT SCHEMATIC

A5-A

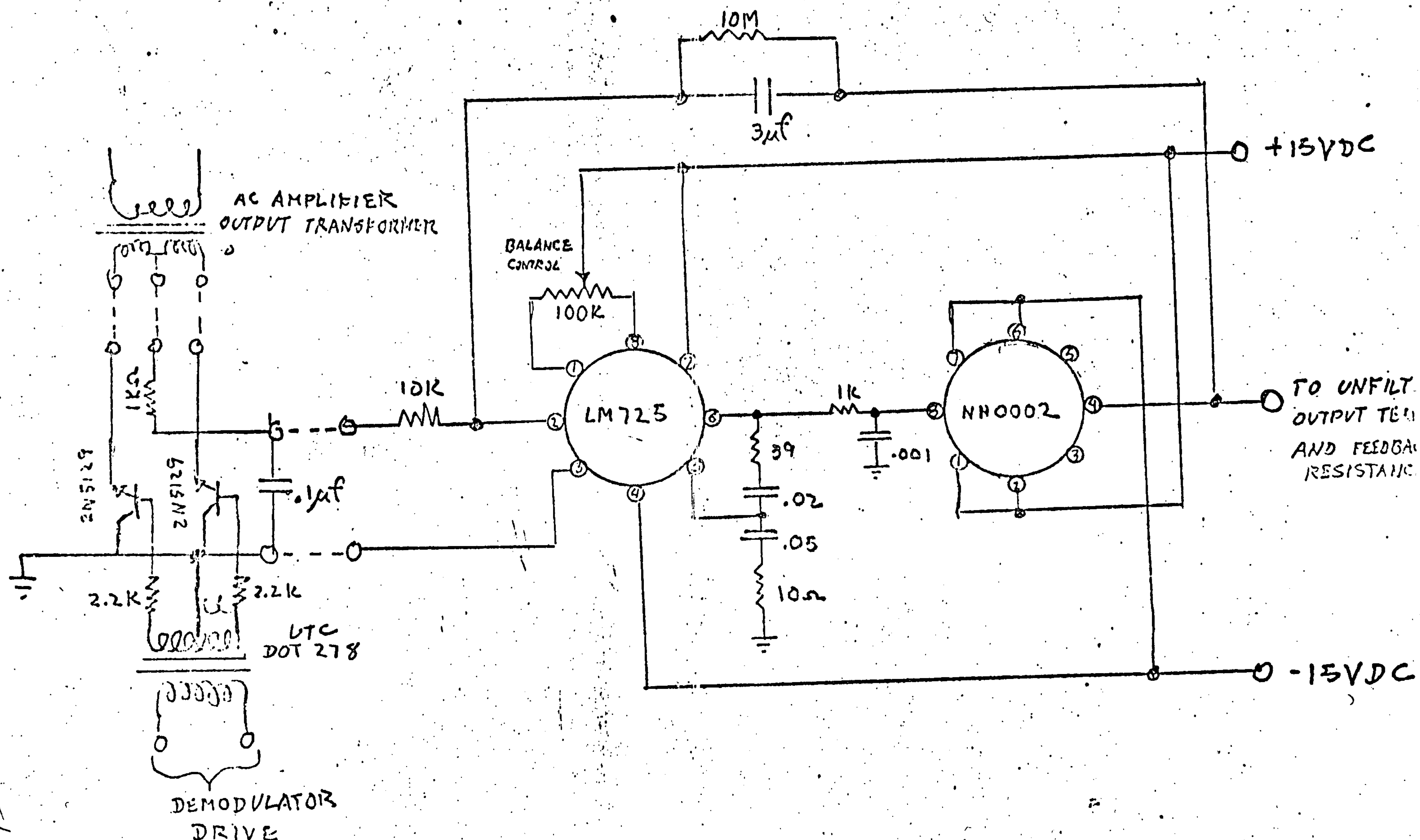

OUTPUT INTEGRATOR AND DEMODULATOR

FIGURE 6.

A-5-6

Operation

Operation of the fluxgate test unit consists of setting the operating frequency, the drive level and the demodulator phase. The drive level is set with a front panel screwdriver adjust while monitoring the drive level at the meter output terminals and the meter function switch in the drive position. A resistance, in series with the drive winding, is mounted on terminals accessible from the rear. The sensor may be operated over a range of drive power levels by varying either or both the drive level adjust and the drive resistor.

Demodulator phase is set by the phase screwdriver adjust on the front panel. This control is adjusted to minimize the amplitude of the signal monitored across the meter terminals with the meter function switch in the AC amp position.

The sensitivity of the sensor is adjusted by the gain screwdriver adjust. This adjustment controls the amount of feedback to the sensor. For a ring core sensor having 2000 turns on the sense winding and 150 turns on the feedback winding the gain may be set from 0.1 volts/gamma to 3.0 volts/gamma. Gain is set by zeroing the sensor output, indicated across the unfiltered output terminals, and then applying a known field the gain adjustment is set for the desired reading.

Performance

The fluxgate test unit has been used to evaluate a number of cores and winding configurations. Stable operation of the cores has been observed for periods up to 24 hours with electronic temperature variations of $\pm10°$ F. Residual noise in the fluxgate test unit has been measured to be less than 2 milligamma equivalent with a shorted input. The overall frequency response, with the gain set at 0.1 volt/gamma was measured to be 10 Hz.

Typical operation is shown by Figure 3 which shows a strip chart recording of a 4-79 ring core, a 2000 turn sense winding and a 200 turn feedback winding.